Songklanakarin J. Sci. Technol.
35 (4), 451-459, Jul. - Aug. 2013

SJST SONGKLANAKARIN JOURNAL OF SCIENCE AND TECHNOLOGY
http://www.sjst.psu.ac.th

Original Article

Removal of methyl orange from aqueous solutions by adsorption using chitosan intercalated montmorillonite

Chakkrit Umpuch[1,2*] and Songsak Sakaew[1]

[1] *Department of Chemical Engineering, Faculty of Engineering,*

[2] *National Center of Excellence for Environmental and Hazardous Waste Management, Ubon Ratchathani University, Warin Chamrap, Ubon Ratchathani, 34190 Thailand.*

Received 13 May 2012; Accepted 3 June 2013

Abstract

Adsorption of methyl orange (MO) using a montmorillonite modified with chitosan has been investigated. The characteristics of montmorillonite and chitosan intercalated montmorillonite (CTS/MMT) were examined by means of SEM and BET-analysis. The effects of operating parameters such as contact time, initial solution pH, initial dye concentration, and temperature on the adsorption of MO were also studied. The results revealed that adsorption of MO was initially rapid and the equilibrium time was reached after 1 hr. Adsorption kinetics were best described by the pseudo-second order model. An aqueous solution with a pH of 2.0 was favorable for the adsorption. The equilibrium data were better fitted by Langmuir isotherm compared to the Freundlich isotherm. The adsorption of MO increased with operating temperatures indicating an endothermic process. Reutilization of the bio-composite was feasible. These results suggested that the CTS/MMT can be used as an adsorbent for removal of MO from aqueous solutions.

Keywords: adsorption, chitosan intercalated montmorillonite, intercalation, methyl orange, desorption

1. Introduction

Accumulation of dyes in wastewater from industries such as textiles, paper, cosmetics, rubber, and plastics has been regarded as a significant source of water pollution. Reactive dyes, an anionic dye, are most commonly used due to their provision of bright colors, excellent color fastness, and easy application (Annodurai *et al.*, 2008). However, many reactive dyes are toxic to organisms and may cause direct harm to aquatic life. As the dyes are structurally complex, are of synthetic origin, and have high water solubility, their removal from effluent by the use of conventional physico-chemical and biological processes is difficult (Salleh *et al.*, 2011). However, it has been reported that the adsorption technique provides a potential for the removal of dyes from aqueous solutions (Crini and Badot, 2008).

The use of natural polymeric matter as an adsorbent, for instance chitosan (CTS), has been gaining interest in wastewater treatment due to its biodegradable and non-toxic nature. CTS, a natural biopolymer, contains amine functions (acid-base properties, solubility, and cationic behavior) and is highly efficient in the removal of anionic dyes (Szygula *et al.*, 2008). However, CTS has some limitations, such as low specific gravity, high solubility obtained only in acidic conditions, and weak mechanical properties, which requires improvements for practical operations (Chiou *et al.*, 2003). To overcome or reduce these drawbacks, the immobilization of CTS on clay minerals, such as montmorillonite clay, to form bio-composite materials has been reported (Wang and Wang, 2007).

Montmorillonite clay (MMT), a natural mineral, which is also found in Thailand, has a lamellar structure which contains permanent negative charges on the clay layers.

* Corresponding author.
Email address: enchakum@ubu.ac.th

MMT normally adsorbs high amounts of cations due to an electrostatic attraction between the permanent negative charges and the cations (Wibulswas, 2004). CTS can be highly adsorbed or intercalated onto MMT. Wang and Wang (2007) reported that CTS/MMT improved the mechanical and material properties of CTS and additionally exhibited a higher adsorption capacity of anionic dyes when compared to CTS and MMT. Kittinaovarat *et al.* (2010) also reported that CTS/MMT provided a higher adsorption capacity of reactive red, an anionic dye, comapred to CTS alone. However, a study of the removal of anionic dyes using CTS/MMT as an adsorbent has not been documented.

In this study CTS/MMT bio-composites were first synthesized and characterized, and then the adsorption kinetics, isotherms, and thermodynamics for MO adsorption from aqueous solutions of CTS/MMT were investigated as a function of contact time, initial solution pH, initial dye concentration, and operating temperature; finally the desorption of MO was studied.

2. Experiment

2.1 Materials

MO (Molecular formula: $C_{14}H_{14}N_3NaO_3S$) obtained from Asia Pacific Specialty Chemicals was used as the adsorbate in this study. CTS (Molecular formula: $C_{12}H_{24}N_2O_9$) of high molecular weight (10,104 g/mol) was provided by Sigma-Aldrich. The MO molecular weight is 327.33 g/mol. Commercial MMT was supplied by Thai Nippon Chemical Industries Co. Ltd., Thailand, and used without further purification. The chemical composition (wt.%) of MMT was SiO_2 (56-60%), Al_2O_3 (16-18%), Fe_2O_3 (5-7%), Na_2O (2.4-3%), MgO (1.5-2.0%), CaO (1.9-2.1%), K_2O_3 (0.3-0.5%) and TiO_2 (1.2-1.5%). The cation exchange capacity (CEC) of MMT was 0.8 meq/g; a value provided by the supplier.

2.2 Preparation of chitosan intercalated montmorillonite

An amount of 1.0 g of MMT was grinded into paste in 100 mL of distilled water then added in 100 mL of 2 g/L CTS solution with constant stirring for 1 hr at 298.2 K. The pH of the suspension was adjusted to 7.0-7.5 using 1 N HCl and aged 30 min to allow for gel formation at 298.2 K (Fan *et al.*, 2006). The CTS/MMT obtained was filtrated with microfiber filter (77 mm) to separate the CTS/MMT complex from the suspension and then washed with distilled water until the pH of washed water became neutral and then dried at 40°C for 12 hrs prior to being ground and sieved through a 200 mesh sieve. The intercalation of CTS onto MMT was confirmed using a CHNS-analyzer.

2.3 Characterization

To get further insight into the MMT and CTS/MMT morphology, the samples were analyzed by scanning electron microscopy (SEM). The specific surface area and average pore size of the adsorbents were determined by nitrogen adsorption at 76 K. The Brunauer Emmett-Teller (BET) method was employed for the corresponding calculation.

2.4 Adsorption experiments

All adsorption experiments were carried out in a thermostat shaker at 200 rpm using flasks of 250 mL. A series of adsorption experiments were carried out in different operating conditions related to contact time, initial solution pH, initial dye concentration, and operating temperature.

The first experiment studied the effect of contact time and equilibrium time on MO uptake. An amount of 0.1 g CTS/MMT dispersed in 100 mL of 200 mg/L MO solution (pH_0 = 7.0±0.5) was horizontally shaken at 298.2 K for various contact times ranging from 5 min to 12 hrs. The second experiment investigated the effect of initial solution pH on MO uptake. The initial pH value of 200 mg/L MO solutions was adjusted to 2.0, 4.0, 6.0, 8.0, and 10.0 with 0.1 N NaOH or 0.1 N HNO_3 solutions. An amount of 0.1 g of CTS/MMT was added to the MO solution in a flask then horizontally shaken for 24 h at 200 rpm (298.2 K). The third experiment studied the adsorption isotherm. About 200 mL of MO solution at different initial concentrations of 50, 100, 150, 200, 250, and 300 mg/L (pH_0 = 7.0±0.5) were prepared and then treated according to the procedure in the second experiment. The final experiment considered the effect of temperature on MO uptake. The experiment was performed according to the procedure in the second experiment, but the temperature was varied from 308.2 to 328.2 K .

All solution samples were centrifuged at 6,000 rpm for 30 min to remove the dye loaded adsorbent from the suspended solution. The MO concentration in supernatant was measured using a UV-Vis-spectrophotometer at wavelength corresponding to the maximum absorbance for MO (520 nm). The concentrations were then determined using linear regression equation obtained by plotting a calibration curve for MO over a range of concentrations.

2.5 Desorption experiments

The MO loaded CTS/MMT obtained from adsorption experiments of 200 mg/L of MO solution (200 mL) with 0.1 g of adsorbent, was collected by filtration and washed with deionized water for three times, then dried in air for one day. The CTS/MMT loaded with MO was treated with 200 mL of 0.1 M NaOH solutions, and shaking at 200 rpm for 24 hrs. It was again filtrated and the desorbed MO was determined in the filtrate. The adsorbent was washed several times with distilled water in order to remove excess base and used for the next desorption cycle. The adsorption-desorption cycle was repeated three times using the same adsorbent.

3. Results and Discussion

3.1 Properties of as received MMT and CTS/MMT

3.1.1 Scanning electron microscopy

Scanning electron micrographs of MMT (Figure 1a) and CTS/MMT (Figure 1b) showed that the presence of CTS rendered lamellar structures where the clay particles appeared to be enveloped in a biopolymer network.

3.1.2 Specific BET surface analysis

Figure 2 gives the nitrogen adsorption-desorption isotherms measured on MMT and CTS/MMT samples. The both isotherms also showed a IUPAC type IV pattern with sharp inflection of nitrogen adsorbed volume at P/P_0 about 0.85 indicating the existence of mesopores in MMT and CTS/MMT samples. The specific BET surface areas of MMT and CTS/MMT were 78.23 m^2/g and 27.95 m^2/g, respectively. The lower surface area of CTS/MMT was attributed to the compact packing of the CTS molecules in the interlayer space, resulting in pore blocking that inhibited the passage of nitrogen molecules. The average pore diameter of CTS/MMT was 8.92 nm compared to 3.62 nm of MMT

3.2 Effect of contact time

The adsorption rate was rapid during the first 5 min and then continued at a slower rate from 5 to 60 min, and almost reached a plateau after approximately 60 min of the experiment (see Figure 3). This was due to the fact that, at the initial stage the number of free adsorption sites was higher, and the slow adsorption rate in the later stage was due to slower diffusion of solute into the interior of the adsorbent. The maximum adsorption occurred after 60 min and there was almost no adsorption beyond this time.

3.3 Effect of temperature

Figure 4 illustrates the adsorption capacity of the bio-composite increased with an increase of the temperature from 298.2 to 328.2 K. It can be seen that higher temperatures were favorable for adsorption. The equilibrium adsorption capacity was affected by temperature, especially, with the amount of MO adsorbed increasing from 53.33 to 95.55 mg/g when the temperature was raised from 298.2 to 328.2 K. It has been well-documented that temperature has two major effects

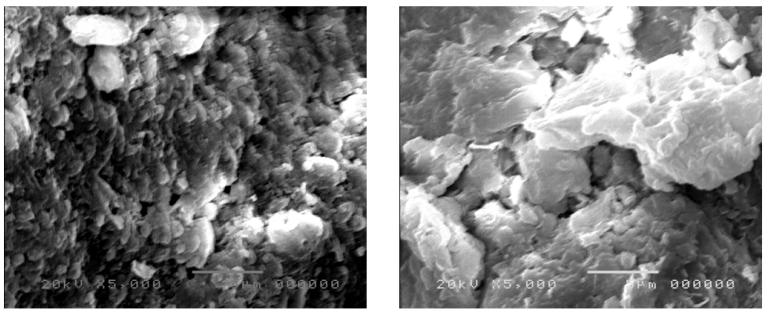

(a) (b)

Figure 1. SEM image of MMT (a) and CTS/MMT (b).

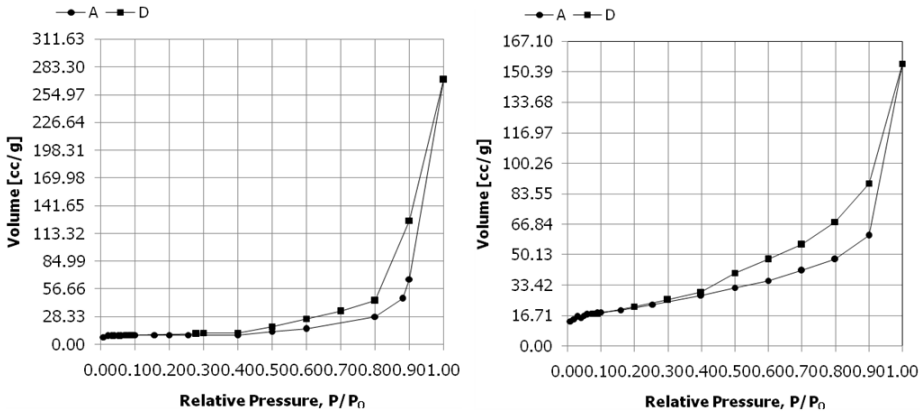

(a) (b)

Figure 2. Nitrogen adsorption-desorption isotherms measured on MMT (a) and CTS/MMT (b) samples.

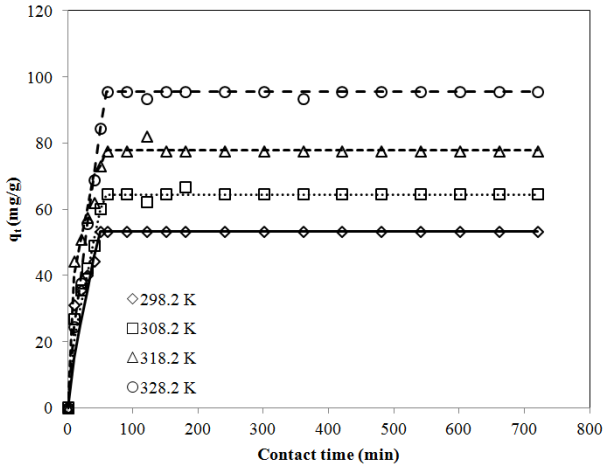

Figure 3. Effect of temperature on the adsorption of MO onto CTS/MMT for a solution initially containing 200 mg/L of CTS/MMT as a function of time.

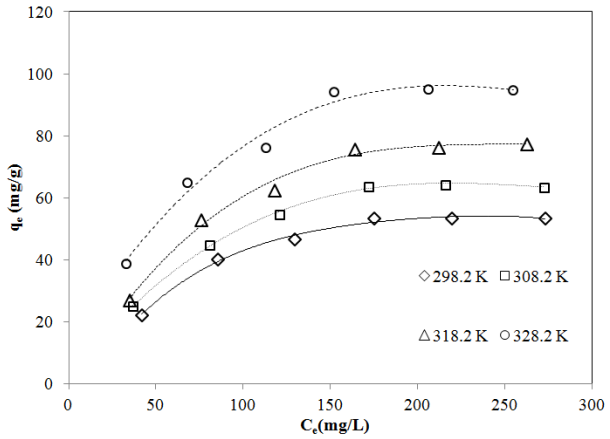

Figure 4. Adsorption isotherm and effect of temperature on the adsorption of MO onto CTS/MMT for a solution initially containing 200 mg/L of CTS/MMT as a function of equilibrium concentration.

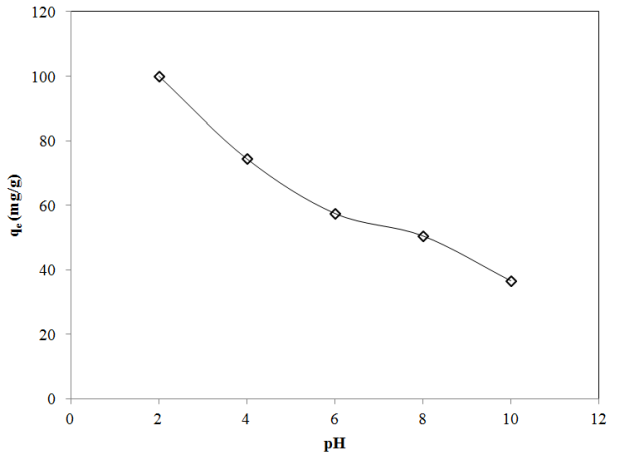

Figure 5. Effect of initial pH solution on the adsorption of MO onto CTS/MMT for a solution initially containing 200 mg/L of CTS/MMT.

on the adsorption process. An increase in temperature is known to increase the rate of diffusion of the adsorbate molecules across the external boundary layer and in the internal pores of the adsorbent particles as a result of the decreased viscosity of the solution (Al-Qodah, 2000). Almeida *et al.* (2009) suggested that a swelling effect within the internal structure of the adsorbent penetrating the large dye molecule is likely to occur when the temperature increased. In addition, Cestari *et al.* (2005) reported that the dimensions of the chitsan pores increased with temperature. The greater the particle pore sizes, the smaller the contribution of intraparticle diffusion resistance. Gunasekar and Ponnusami (2012) reported the adsorption of methylene blue by carbonized plant leaf powder was the endothermic physisorption. Therefore, it can be concluded that the adsorption of MO onto CTS/MMT is an endothermic process, which involves physical changes of the CTS/MMT.

3.4 Effect of initial solution pH

Figure 5 shows the influence of the pH of the initial dye solution on the adsorption capacity of MO on CTS/MMT. As the pH value increased from 2.0 to 6.0, the adsorption capacity of dye onto CTS/MMT rapidly decreased from 100 to 57.5 mg/g. It then slowly decreased from 57.5 to 36.5 mg/g with a further increase of the pH from 6.0 to 10.0. The decrease of the adsorbed dye capacity was attributed to two mechanisms, firstly, an electrostatic attraction between the protonated amino groups of CTS and the dyes, and secondly, the chemical interaction between MO and CTS/MMT (Wang and Wang, 2007). At lower pH values more protons were available causing an increase in electrostatic attraction between negative charge dye anions and positive charge amine groups on CTS/MMT. This resulted in an increase in dye adsorption capacity. As the initial pH of the solution increased, the positive charge on the surface decreased and the number of negative charge sites increased. The negative charge surface sites on the clay were not favorable to the adsorption anionic dye due to electrostatic repulsion. Moreover, there was a competition between the hydroxide ions and the dye anions. The repulsion between anionic dye molecules and the excessive hydroxide ions resulted in a sharp decrease in adsorption. However, the significant adsorption of the anionic MO dye on CTS/MMT still occurred in alkaline medium (Almeida *et al.*, 2009) due to the fact that a chemical interaction between MO dye and CTS/MMT took place.

3.5 Adsorption isotherms

The amount of MO adsorbed at a state of equilibrium (q_e) (mg/g) was calculated using the following equation (Almeida *et al.*, 2009):

$$q_e = V(C_0 - C_e)/m \quad (1)$$

where C_0 (mg/L) is the initial MO concentration, C_e (mg/L) the equilibrium concentration of MO solution, V (L) the volume of MO solution, and m (g) is the mass of adsorbent. The Langmuir isotherm is valid for monolayer adsorption onto a surface with a finite number of identical sites (Chen *et al.*, 2011). If MO adsorption conforms to the Langmuir model, the adsorption process can be expressed as:

$$C_e/q_e = 1/(K_L.q_m) + C_e/q_m \quad (2)$$

where q_m (mg/g) is the maximum adsorption capacity and K_L (L/g) is the Langmuir constant related to the adsorption equilibrium. The essential characteristics of the Langmuir isotherm can be expressed by means of 'R_L' a dimensionless constant referred to as the separation factor or equilibrium parameter (Wang and Wang, 2007). The R_L is defined as:

$$R_L = 1/(1+K_L.C_0). \quad (3)$$

This parameter suggests the type of isotherm to be irreversible (R_L=0), favorable (0<R_L<1), linear (R_L=1), or unfavorable (R_L>1). As can be seen from Table 1, at all temperatures the R_L values are between 0 and 1.0, indicating that the adsorption of MO onto CTS/MMT is favorable.

The Freundlich model is usually adopted for heterogeneous adsorption (Iqbal *et al.*, 2009). One of its limitations is that the amount of adsorbed solute increases indefinitely with the concentration of solute in the solution. This isotherm can be described as:

$$\ln q_e = \ln K_F + (1/n) \ln C_e \quad (4)$$

where K_F ($mg^{1-1/n}.L^{1/n}/g$) and n are the physical constants of the Freundlich isotherm, K_F and n are indicators of an adsorption capacity and an adsorption intensity respectively, and n being a constant representing the mutual interaction of adsorbed species. Experimental values of n are usually greater than unity and this means that the forces between the adsorbed molecules are repulsive. In addition, the closer the n value of the Freundlich sorption equations is to zero, the more heterogeneous is the system (Anwar *et al.*, 2010).

Figure 4 shows adsorption isotherms of MO adsorbed onto CTS/MMT. These equilibrium data were fitted to the Langmuir and Freundlich models. The isotherm parameters for the adsorption of MO onto CTS/MMT obtained are listed in Table 1. The results show the Langmuir isotherm to be most appropriate for MO indicating that the monolayer of dye molecules covers the CTS/MMT surface. It can also be seen in Table 1 that the monolayer capacity of adsorbed MO onto CTS/MMT increased with the operating temperatures.

3.6 Thermodynamic studies

In the practical application of a process, the thermodynamic parameters including change in the enthalpy ($\Delta H°$), entropy ($\Delta S°$), and Gibbs free energy ($\Delta G°$) are essential for a further understanding of the effect of temperature on adsorption indicating whether the adsorption processes occurs spontaneously. The effect of temperature on adsorption in this study was investigated at four temperatures (298.2, 308.2, 318.2 and 328.2 K). The values of $\Delta H°$ and $\Delta S°$ were estimated from the slope and intercept of the van't Hoff plot of ln (K_L) versus $1/T$ according to Equation 5. The value of $\Delta G°$ can be determined by Equation 6:

$$\ln K_L = \ddot{A}S^0/R - \ddot{A}H^0/RT \quad (5)$$

$$\Delta G^0 = -RT \ln K_L \quad (6)$$

where R (8.314 J/(mol.K)) is the universal gas constant and T (K) is the absolute solution temperature.

As seen in Table 2, the $\Delta G°$ values are negative for all the experimental temperatures indicating that MO adsorbed onto CTS/MMT was spontaneous and that the system did not gain energy from an external source. When the temperature increased, the magnitude of $\Delta G°$ shifted to a high negative value suggesting that the adsorption was more spontaneous at a higher temperature. In adsorption processes, a $\Delta G°$ value in the range -20 to 0 kJ/mol correspond to spontaneous physical processes, while with a value in the range of -80 to -40 kJ/mol corresponds to chemisorption (Seki and Yurdakoç, 2006). As $\Delta G°$ changed from -17.50 to -14.27 kJ/

Table 1. Isotherm constants and correlation coefficients for the adsorption of MO on CTS/MMT at different temperatures.

Model		T(K)			
		298.2	308.2	318.2	328.2
Langmuir isotherm	q_{max} (mg/g)	70.42	81.30	99.01	123.46
	K_L (L/g)	0.9656	1.196	1.344	1.834
	R_L	0.1956	0.1847	0.1972	0.1833
	r^2	0.9752	0.9789	0.9824	0.9809
Freundlich isotherm	K_F ($mg^{1-1/n}.L^{1/n}/g$)	4.373	5.717	6.002	7.930
	n	2.131	2.230	2.111	2.132
	r^2	0.8914	0.9148	0.9411	0.9276

Table 2. Thermodynamic parameters for the adsorption of MO onto the CTS/MMT.

T(K)	K_L (L/mol)	ΔG^0 (kJ/mol)	ΔH^0 (kJ/mol)	ΔS^0 (kJ/(mol.K))
298.2	316.08	-14.27	+16.55	+0.055
308.2	391.45	-15.30		
318.2	439.90	-16.10		
328.2	600.17	-17.50		

mol when the temperature increased from 298.2 to 328.2K, it can be concluded that the adsorption mechanism is dominated by physisorption (Seki and Yurdakoç, 2006). A positive value of $\Delta H°$ indicates that the adsorption reaction of MO is an endothermic process, as has been found in most cases (Seki and Yurdakoç, 2006; Almeida *et al.*, 2009). This also suggests that a large amount of heat is consumed to transfer MO from an aqueous into a solid phase. The positive value of entropy change ($\Delta S°$) corresponds to an increase in the degree of freedom of the adsorbed species. A small change in the entropy shows that CTS/MMT does not significantly change.

3.7 Adsorption kinetics

The kinetic data were analyzed by applying pseudo-first-order, pseudo-second-order, and intra-particle diffusion models to gain a better understanding of the adsorption process. The q_t (mg/g) is the amount of dye adsorbed at time t calculated from Equation 1 though C_t (the concentration of dye solution at time t) is used instead of C_e. The pseudo-first order kinetic model is the earliest known in describing the adsorption rate based on the adsorption capacity (Lagergren and Svenska, 1898). The pseudo-first-order rate is generally expressed as follows:

$$\ln (q_e - q_t) = \ln q_e - k_1 t \quad (7)$$

where k_1 (1/min) is the rate constant of first-order adsorption. The pseudo-first-order equation does not fit well for the whole range of contact time and is in generally applicable only over the initial 20-30 min of the adsorption process. The pseudo-second-order kinetic model was proposed by Ho in 1995 (Ho and McKay, 1998). The fitting of experimental data and second-order kinetic expression for the adsorption systems of dye ions using CTS/MMT was obtained in which the chemical interaction between the adsorbate-adsorbent on the external surface was the rate-limiting step. It is expressed as:

$$t/q_t = 1/(k_2 . q_e^2) + t/q_e \quad (8)$$

where k_2 (g/(mg.min)) is the rate constant of second-order adsorption. If the diffusion of MO molecules into internal surfaces of pores and capillaries of the adsorbent is the rate-limiting step, the adsorption data can be presented by the following equation (Tunali *et al.*, 2006):

$$q_t = k_i t^{1/2} + C \quad (9)$$

where k_i (mg/(g.(min$^{1/2}$))) represents the intra-particle diffusion rate constant and C is a constant (mg/g) which gives information about the thickness of the boundary layer. The plot of q_t versus $t^{1/2}$ yields a straight line passing through the origin in the case of intra-particle diffusion.

According to Equation 8, the plot of t/q_t against t should be linear. The pseudo-second-order rate constant k_2 and the corresponding linear regression correlation coefficient values, r^2, are given in Table 3. The high values of r^2 (0.9988-0.9998) for all temperatures indicate that the adsorption data fit well to the pseudo-second-order kinetics for the entire adsorption process. As seen in Table 3, the adsorption data were found to conform to the pseudo-second-order model. This indicated that the rate of limiting step was the interaction between the MO ions and protonated amine groups, which can bind the dye anions to the CTS/MMT surfaces. Table 3 shows that the rate constant decreases as the temperature increases. This is only to be expected in conventional physisorption systems (Tunali *et al.*, 2006).

According to Equation 7 and 9, a straight line should be obtained from both plotting of ln (q_e-q_t) versus t and of q_t versus $t^{1/2}$. However, neither equation fitted well for the whole range of concentrations at any contact times exhibiting poor correlation coefficient values. Accordingly, the experimental data did not conform to either of these models.

3.8 Activation parameters

It is possible to gain some insight into the type of adsorption from four of the pseudo-second-order rate constants, k_2, each at a different temperature, and using the Arrhenius equation (Equation 10):

$$\ln k_2 = \ln A - E_a/RT \quad (10)$$

where E_a is the activation energy (kJ/mol), k_2 is the pseudo-second-order rate constant for adsorption (g/(mol.s)), A is the temperature-independent Arrhenius factor (g/(mol.s)), R is the gas constant (8.314 J/(K.mol)), and T is the solution

Table 3. Pseudo-first order, pseudo-second and intra-particle diffusion kinetic parameters for MO adsorbed on CTS/MMT.

Model		T(K)			
		298.2	308.2	318.2	328.2
	q_e (exp) (mg/g)	53.33	63.33	77.78	95.56
Pseudo- first	k_1 (1/min)	0.0416	0.0516	0.0549	0.0448
Order	q_e (cal) (mg/g)	48.87	68.92	77.87	115.13
	r^2	0.9303	0.8945	0.9037	0.9233
Pseudo-second	k_2 (g/(mg.min))	0.00465	0.00337	0.00327	0.00243
Order	k_2 (g/(mol.s))	25.36	19.09	17.84	13.27
	q_e (cal) (mg/g)	53.76	64.10	78.13	97.09
	r^2	0.9998	0.9998	0.9998	0.9988
Intra- particle	k_i (mg/(g.(min$^{1/2}$)))	0.590	0.838	0.882	1.764
diffusion	C (mg/g)	41.35	45.99	59.93	59.70
	r^2	0.4402	0.4339	0.4260	0.4294

temperature (K). The slope of the plot of ln k_2 vs. $1/T$ can then be used to evaluate E_a.

The experimental results showed that E_a = -16.35 kJ/mol for the adsorption of MO onto CTS/MMT (see Figure 6). The negative value of the activation energy suggested that the rates of adsorption decrease with an increase in the solution temperature. The negative activation energy also indicates that energy barriers are absent in the adsorption process. It can be described that an increase the temperature leads to a reduction in the probability of the colliding molecules capturing one another and this results in a negative activation energy (Kobiraj *et al.*, 2012). The low value of the activation energy (E_a < 42 kJ/mol) indicates that the adsorption process of MO adsorption onto CTS/MMT might be a physical adsorption. It means that the rate-limiting step of MO adsorption onto CTS/MMT involved predominantly a physical process such as diffusion process (Chiou and Li, 2003; Chiou *et al.*, 2003; Al-Ghouti *et al.*, 2005).

3.9 Desorption of MO

Desorption experiments were carried out as described in Section 2.5. After the third desorption cycle, the desorption efficiency is decreased from 92.94% to 81.05% (see Figure 7). A complete desorption of MO ions could not be obtained, which might be due to MO ions becoming trapped in the intrapores and, therefore, difficult to release (Vijayaraghavan and Yun, 2008). As a physisorbed molecule usually can be easily desorbed, thus indicating a weak intercalation between MO and CTS/MMT surface. As the alkaline solution can desorb the dye, it could be said that the attachment of the dye onto the adsorbent is by ion exchange. Moreover, the quantity of desorption is always greater than the following adsorption capacity. It is attributed to the employed regeneration technique that may cause any detrimental effects to the adsorbent structure, which might lower the sorption capacity.

4. Conclusion

The CTS/MMT exhibited good adsorption capacity for the removal of MO from aqueous solutions. The adsorption was depending on contact time, initial solution pH, and

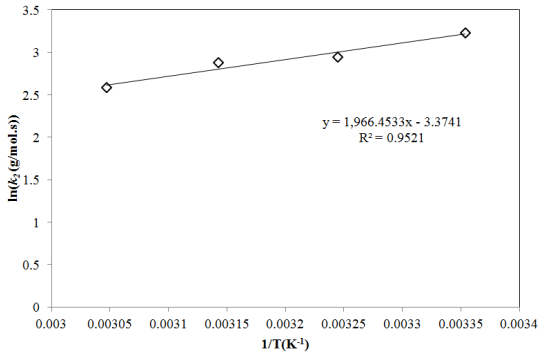

Figure 6. Plot of ln k_2 versus $1/T$: estimation of the activation energy, E_a, for the adsorption of MO onto CTS/MMT.

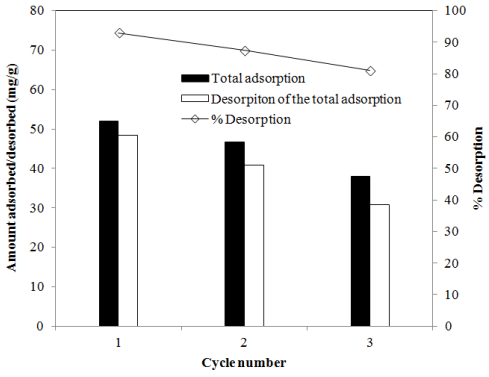

Figure 7. Reuse of the CTS/MMT for adsorption of MO ions (initial MO concentration: 200 mg/L; mass of CTS/MMT: 0.1 g; initial pH 7.0; desorption solution: 200 mL of 0.1M NaOH).

temperature. The adsorption equilibrium was attained within 60 min and the maximum adsorption was obtained at the initial solution pH of 2.0 and temperature at 328.23 K. The equilibrium data obtained at different temperatures fitted well with the Langmuir model. The maximum monolayer capacity of MO adsorbed onto CTS/MMT increased from 70.42 to 123.46 mg/g when the temperature increased from 298.2 to 328.2 K, showing that the uptake of MO increased with operating temperature. The calculated values of ΔH^0, ΔS^0 and ΔG^0 suggested that the adsorption was endothermic, random, and spontaneous. Regarding kinetic studies, the pseudo-second order kinetic model agreed with the dynamic behavior for the adsorption of MO onto CTS/MMT, with activation energy of -16.35 kJ/mol. The desorption experiment indicated that the CTS/MMT can be reused. Though the results from the effect of initial solution pH and kinetic experiments reveal the adsorption process is chemisorptions, others support physisorption. Therefore, the adsorption process might involve both chemisorption and physisorption. These results suggested that CTS/MMT is a potential adsorbent for the reduction of dye accumulations normally found in the effluent of various industries.

Acknowledgments

This work was financially supported by the Environmental Engineering Program in the Department of Chemical Engineering, Faculty of Engineering, Ubon Ratchathani University. The authors express their sincere gratitude to C. Kunyawut for useful and detailed comments, and to B. Tremayne, from the Division of International Relations at Ubon Ratchathani University, for assistance with English.

References

Al-Ghouti, M., Khraisheh, M.A.M., Ahmad, M.N.M. and Allen, S. 2005. Thermodynamic behavior and the effect of temperature on the removal of dyes from aqueous solution using modified diatomite: A kinetic study. Journal of Colloid and Interface Science. 287, 6-13.

Almeida, C.A.P., Debacher, N.A., Downs, A.J., Cottet, L. and Mello, C.A.D. 2009. Removal of methylene blue from colored effluents by adsorption on montmorillonite clay. Journal of Colloid and Interface Science. 332, 46-53.

Al-Qodah, Z. 2000. Adsorption of dyes using shale oil ash. Water Research. 34, 4295-4303.

Annodurai, G., Ling, L.Y. and Lee, J.-F. 2008. Adsorption of reactive dye from an aqueous solution by chitosan: isotherm, kinetic and thermodynamic analysis. Journal of Hazardous Materials. 152, 337–152,346.

Anwar, J., Shafique, U., Zaman, W.-U., Salman, M., Dar, A. and Anwar, S. 2010. Removal of Pb(II) and Cd(II) from water by adsorption on peels of banana. Bioresource Technology. 101, 1752-1755.

Cestari, A.R., Vieira E.F.S., Pinto, A.A. and Lopes E.C.N. 2005. Multiple adsorption of anionic dyes on silica/chitosan hybrid 1. Comparative kinetic data from liquid- and solid-phase models. Journal of Colloid and Interface Science. 292, 363-372.

Chen, D., Chen, J., Luan, X., Ji, H. and Xia, Z. 2011. Characterization of anion-cationic surfactants modified montmorillonite and its application for the removal of methyl orange. Chemical Engineering Journal. 171, 1150–1158.

Chiou, M.-S., Kuo, W.-S. and Li, H.-Y. 2003. Removal of reactive dye from wastewater by adsorption using ECH cross-linked chitosan beads as medium. Journal of Environmental Science and Health. A38, 2621-2631.

Chiou, M.-S. and Li, H.-Y. 2003. Equilibrium and kinetic modeling of adsorption of reactive dye on cross-linked chitosan beads. Journal of Hazardous Materials. B93, 233-248.

Crini, G. and Badot, P.-M. 2008. Application of chitosan, a natural aminopolysaccharide, for dye removal from aqueous solutions by adsorption processes using batch studies: A review of recent literature. Progress in Polymer Science. 33, 399–347.

Gunasekar, V. and Ponnusami, V. 2013. Kinetics, equilibrium, and thermodynamic studies on adsorption of methylene blue by carbonized plant leaf powder. Journal of Chemistry (in press).

HO, Y.S. and McKay, G. 1998. Sorption of dye from aqueous solution by peat. Chemical Engineering Journal. 70, 115-124.

Iqbal, M., Saeed, A. and Zafar, S. I. 2009. FTIR spectrophotometry, kinetics and adsorption isotherms modeling, ion exchange, and EDX analysis for understanding the mechanism of Cd^{2+} and Pb^{2+} removal by mango peel waste. Journal of Hazardous Materials. 164, 161-177.

Kittinaovarat, S., Kansomwan, P. and Jiratumnukul, N. 2010. Chitosan/modified montmorillonite beads and adsorption Reactive Red 120. Applied Clay Science. 48, 87-91.

Kobiraj, R., Gupta, N., Kushwaha, A.K. and Chattopadhyaya, M.C. 2012. Determination of equilibrium, kinetic and thermodynamic parameters for the adsorption of Brilliant Green dye from aqueous solutions onto eggshell powder. Indian Journal of Chemical Technology. 19, 26-31.

Lagergren, S. and Svenska, B.K. 1898. About the theory of so-called adsorption of soluble substances. Vaternskapsakad Handlingar. 24(4), 1-39.

Salleh, M.A.M., Mahmoud, D.K., Karin, W.A. and Idris, A. 2011. Cationic and anionic dye adsorption by agricultural solid wastes: A comprehensive review. Desalination. 280, 1-13.

Seki, Y. and Yurdakoç, K. 2006. Adsorption of Promethazine hydrochloride with KSF Montmorillonite. Adsorption. 12(1), 89-100.

Szygula, A., Guibal, E., Ruiz, M. and Sastre, A.M. 2008. The removal of sulphonated azo-dyes by coagulation with chitosan. Colloids and Surfaces A: Physicochemical and Engineering Aspects. 330, 219-226.

Tunali, S., özcan, A.S. özcan, A. and Gedikbey, T. 2006. Kinetics and equilibrium studies for the adsorption of acid red 57 from aqueous solution onto calcined-alunite. Journal of Hazardous Materials. 135, 141-148.

Vijayaraghavan, K. and Yun, Y.-S. 2008. Bacterial biosorbents and biosorption. Biotechnology Advances. 26, 266–291.

Wang, L. and Wang, A. 2007. Adsorption characteristics of Congo Red onto the chitosan/montmorillonite nanocomposite. Journal of Hazardous Materials. 147, 979-985.

Wibulswas, R. 2004. Batch and fixed bed sorption of methylene blue on precursor and QACs modified montmorillonite. Separation and Purification Technology. 39, 3-12.